Electronic Supplementary Information

Calix[4]arene@MIL-101 as host@MOF for cage-in-cage pore space partitioning for enhanced CO_2 separation and catalysis

Saied Shafiei Navid,[a,b] Rahman Hosseinzadeh,*[a] Robert Oestreich,[b] Soheil Abdpour,[b] Thi Hai Yen Beglau,[b] Christoph Janiak*[b]

[a] Department of Organic Chemistry, Faculty of Chemistry, University of Mazandaran, Babolsar,

Iran

Emails: s.shafiei@stu.umz.ac.ir, r.hosseinzadeh@umz.ac.ir

[b] Institut für Anorganische Chemie und Strukturchemie, Heinrich-Heine-Universität Düsseldorf 40225 Düsseldorf, Germany.

Emails: Robert.Oestreich@hhu.de, soabd100@uni-duesseldorf.de, beglau@uni-duesseldorf.de, janiak@hhu.de

*Corresponding authors

Prof. Rahman Hosseinzadeh

E-mail address: r.hosseinzadeh@umz.ac.ir

Tel.: +98-11-35302356.

Prof. Christoph Janiak

E-mail address: : janiak@hhu.de

Tel.: 0211-81-12286

Table of Contents

1. Materials

All the solvents and chemicals were purchased from commercial vendors and were used as delivered. *p*-*tert*-butyl-calix[4]arene (95%), *N*,*N*-dimethylformamide (DMF, 99.8%), nitric acid (HNO_3, 65 wt%), hydrochloric acid (HCl, 37 wt%), ethanol (EtOH, 99.5%), terephthalic acid (H_2BDC, 98%) were obtained from Sigma-Aldrich. $Cr(NO_3)_3 \cdot 9H_2O$ (99%), maleic acid (MA, 99.99%), 4-*tert*-butylphenol (99%), and formaldehyde (37 wt%) were purchased from Merck (Darmstadt, Germany).

2. Instruments and Methods

Powder X-ray diffraction patterns (PXRD) were recorded on a Bruker D2 Phaser powder diffractometer equipped with a flat silicon low-background sample holder using Cu-Kα radiation (λ = 1.5418 Å, 30 kV, 10 Ma, ambient temperature). All samples were measured over the 2θ range of 2-50° with a scan speed of 2° min^{-1} at room temperature. Simulated patterns of MIL-101 were calculated using the CCDC Mercury 3.7 program using the respective single crystal data (CCDC ref. code OCUNAC, CSD-605510).

Fourier-transform infrared spectra (FT-IR) were recorded using a Bruker Tensor 37 instrument using in attenuated total reflection (ATR) mode in the range of 600-4000 cm^{-1}.

Elemental analyses regarding C, H, N, and S were carried out on an Elementar Vario EL III analyzer.

Thermogravimetric analysis (TGA) was carried out using a Netzsch TG 209 F3 Tarsus in the range of 30°C to 950°C with a heating rate of 10 K min^{-1} using an N_2 carrier gas.

Nitrogen sorption measurements at 77 K were carried out using a Micrometrics ASAP 2020 gas sorption analyzer. Before the measurement, the samples were evacuated and activated at 433 K in a vacuum for 24 hours. The Brunauer-Emmett-Teller (BET) surface areas were calculated in the P/P_o range of 0.05-0.2 using the ASAP 2020 v3.05 software. Total pore volumes were calculated from nitrogen adsorption isotherms at $P/P_0 = 0.9$. The pore size distributions were obtained using Nonlocal Density Functional Theory (NLDFT) calculations, using the model of nitrogen on carbon and slit pores.

CO_2, N_2, and CH_4 adsorption isotherms for MIL-101 and the derived composite materials were recorded using a Quantachrome Autosorb IQ MP automatic adsorption analyzer and measured at 293 K and 273 K (ice/deionized water bath). The neat SCA sample was not analyzed due to very low porosity. All gases were of ultrapure grades (99.999%) supplied by Air Liquide Germany and used as received.

SEM images of samples were recorded with a Jeol JSM-6510LV QSEM Advanced electron microscope with a LaB_6 cathode at 20 keV. The samples were prepared for SEM microscopy by coating them with gold using a JEOL JFC 1200 fine-coater.

The ^1H NMR were performed at an AVANCE III Bruker Biospin spectrometer, operating at 300 MHz.

The products obtained from the catalytic reaction were separated and identified by GC-MSD and GC-QTOF.

The composites were prepared using a digital orbital Shaker and centrifuged by a SR1X3 centrifuge instrument.

Virial analysis for heat of adsorption for CO_2

To calculate the isosteric heat of adsorption (Q_{st}) for CO_2 isotherm data the fitting of the data by the virial equation of state at 273 K and 293 K was used:

$$\ln(P) = \ln(n) + \frac{1}{T}\sum_{i=0}^{m} a_i n^i + \sum_{j=0}^{m} b_j n^j \qquad \textbf{(1)}$$

where P is the pressure in kPa, n is the total amount adsorbed in mmol g^{-1}, T is the temperature in K (273K or 293K), a_i and b_i are the fitted virial coefficients, and n represent quantity adsorbed.

With the established virial coefficents, the Q_{st} is calculated from equation (eq. 2), where R is the universal gas constant.

$$Q_{st} = -\mathrm{R}\sum_{i=0}^{m} a_i n^i \qquad \textbf{(2)}$$

IAST calculations

The gas adsorption selectivity in a mixture of two gases (*i.e.* CO_2/N_2) was calculated according to the ideal adsorption solution theory (IAST) using SIPS (eq. 3) fitted gas adsorption isotherm data for pure gases. 3P sim software (3P Instruments, Germany, version 1.1.0.7) was used to calculate the maximal loadings of each gas depending on the given molar ratio.

$$q_{eq} = q_{max} \cdot \frac{(K_1 \cdot p)^t}{1+(K_1 \cdot p)^t t} + \qquad \textbf{(3)}$$

IAST selectivities *S* of binary gas mixtures were calculated using equation 4,

$$S = \frac{x_1/x_2}{y_1/y_2} \qquad \textbf{(4)}$$

where x_i represents the absorbed gas amount and y_i the mole fraction of each adsorptive.

3. Synthesis

3.1. Synthesis of SCA

The SCA was synthesized based on the method reported by Tauran et al[1]. 2.0 g of *p*-*tert*-butyl-calix[4]arene was slowly added to 20 mL of concentrated sulfuric acid and heated overnight at 80 °C. After cooling, the dark mixture was added to 100 mL of cold diethyl ether and the formed solid was filtered. Then the solid was washed in 100 mL of cold acetone and then filtered and dried at 60 °C in a vacuum oven to yield (1.1 g, 95%) $1^2,3^2,5^2,7^2$-tetrahydroxy-1,3,5,7(1,3)-tetrabenzenacyclooctaphane-$1^5,3^5,5^5,7^5$-tetrasulfonic acid (SCA, Scheme S1).

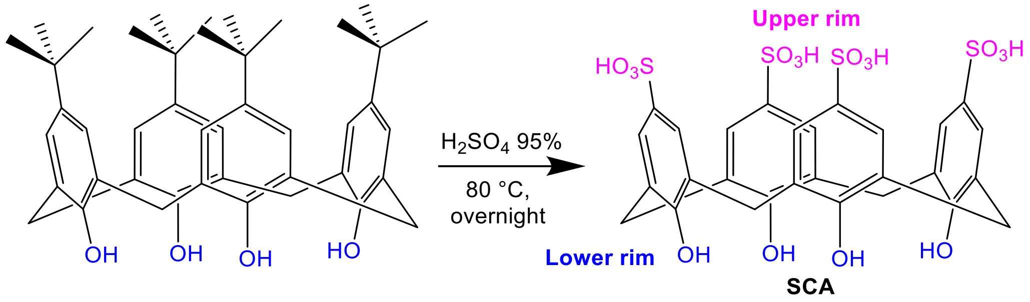

Scheme S1. Preparation of the SCA molecule.

^{1}H-NMR: 3.97 ppm (8H, CH_2, s) and 7.51 ppm (8H, Ar, s).

FT-IR: 3420, 2950, 2890, 1700, 1653, 1462, 1225, 1041, and 634 cm^{-1}.

Elemental analysis data for SCA, calculated for $C_{28}H_{24}O_{16}S_4$: C 45.16%, H 3.42%, S 17.22%; found C 44.12%, H 3.25%, S 16.76%.

3.2. Synthesis of MIL-101(Cr) (MIL-101)

Chromium(III) nitrate nonahydrate ($Cr(NO_3)_3 \cdot 9H_2O$; 3.84 g, 9.6 mmol), benzene-1,4-dicarboxylic acid (H_2BDC; 1.62 g, 9.8 mmol) were stirred in 50 mL of H_2O, followed by the addition of concentrated nitric acid (HNO_3, 65% aq; 0.45 mL, 9.8 mmol) and further stirring for another few minutes. The homogenous mixture was transferred to a PTFE/Teflon liner of an autoclave. The closed autoclave was heated at 200 °C for 15 h and cooled to room temperature. The solid was isolated by centrifugation. The supernatant liquid phase was discarded and the isolated solid was purified by repeated treatment with DMF and ethanol and subsequent isolation by centrifugation. First, it was shacked slowly in 45 mL of DMF for three hours at room temperature, then in 45 ml of DMF for 16 h, followed by shaking in 45 ml of ethanol for three hours, and finally in 50 mL of ethanol for 24 h. The isolated washed solid was dried for one day in air at room temperature, homogenized by minimal careful grinding and activated in two steps: first for 6 hours at 60 °C (~20 Torr), and finally activated at 150 °C (10^{-2} Torr) for 20 hours. The activated material was stored under nitrogen atmosphere. Yield 2.43 g (65 % with respect to chromium)[2].

For the synthesis of the SCA@MIL-101-*w* composites see Section 3.3 in the main text.

3.3. Catalytic activity of SCA@MIL-101-*30*

The SCA@MIL-101-*30* was synthesized as mentioned in the manuscript and washed with excess amount of deionized water and ethanol (Figures S27 and S28). Finally, the SCA@MIL-101-*30* were activated at 150 °C under vacuum overnight (~20 Torr) before using as a catalyst. To assess the catalytic activity, the reactions were performed in a thick-walled vials thermostat which was treated with 20 mg of the activated SCA@MIL-101-*30*, a mixture of carboxylic acid and alcohol (substrates, Table 3) at 120 °C in a homemade aluminum block (Figure S29) for 4 h. After the completion of the reaction and to obtain the conversion yield, the mixture was analyzed with a GC/MS instrument, without any prior processing. The reusability of the SCA@MIL-101-*30* catalyst was studied after washing the catalyst with excess amount of water and ethanol and pre-dried at 60 °C and activated at 150 °C overnight at ~20 Torr.

To assess the acidity strength of the prepared composite, in a typical procedure 25 mg of the composite was suspended in 1 mL of saturated NaCl aqueous solution and the mixture was then stirred at room temperature for about 10 h. The filtrate pH value was measured with a pH-meter. The obtained pH value was <1.0 which indicated that the composite material has a relatively high acidity to use as a Brønsted acid for esterification reaction.[3]

3.4. ^{1}H NMR-based determination of the SCA content in SCA@MIL-101

To prove the successful synthesis of SCA@MIL-101(Cr) composites, the SCA content was established in the centrifugate by ^{1}H NMR spectroscopy using maleic acid (MA) as an internal standard (see Section 3.4a) and an isolated and activated sample with determined weight was subjected to decomposition ("digestion") (Section 3.4b).

a) Analysis of supernatant SCA solution:

The actually adsorbed amounts of SCA were measured by determining the amount of the latter remaining in the supernatant after the adsorption (Table S1). The determination was carried out by quantitative ^{1}H NMR using maleic acid (10 mg) as an internal standard which was added. The adsorbed amount was determined by subtraction of the amount left in the supernatant from the initial amount added. The obtained data essentially represents an adsorption isotherm of SCA by MIL-101 at room temperature, with high-excess values asymptotically nearing the maximum capacity. The ^{1}H NMR spectrum of SCA shows two peaks at $\delta = 4.0$ and 7.5 ppm, which are attributed to the bridging methylene- and aromatic protons, respectively (Fig. S1).[4] The ^{1}H NMR spectra of the supernatant of the composites are shown in Fig. S2 to Fig. S4, with the maximum amount of incorporated SCA reached, as expected, for the highest initial amounts used (30 mg of SCA and 10 mg of MIL-101 (Table S1)); while the incremental increase of the loading was very small at the last step of excess increase, hence, it was assumed that it is a good estimate of the adsorptive capacity and no larger excesses were checked.

Table S1. Determination of the SCA content in the SCA@MIL-101 composites using ^{1}H NMR of the supernatant samples with maleic acid as an internal standard.

Sample	I_{MA}	I_{SCA}	M_{MIL} (mg)	Incorporated SCA (mg)	Incorporated SCA (wt. %)
SCA@MIL-101-*5*	1.00	0.15	10	3.72	27
SCA@MIL-101-*10*	1.00	0.25	10	5.99	37
SCA@MIL-101-*25*	1.00	0.39	10	9.89	50
SCA@MIL-101-*30*	1.00	0.41	10	10.29	50

I_{MA}: relative integral of the MA proton peak in the ^{1}H NMR spectrum, I_{SCA}: relative integral of the SCA aromatic proton peak in the ^{1}H NMR spectrum. SCA (wt. %): the SCA weight percent in the SCA@MIL-101 composites, obtained from the ^{1}H NMR calculation.

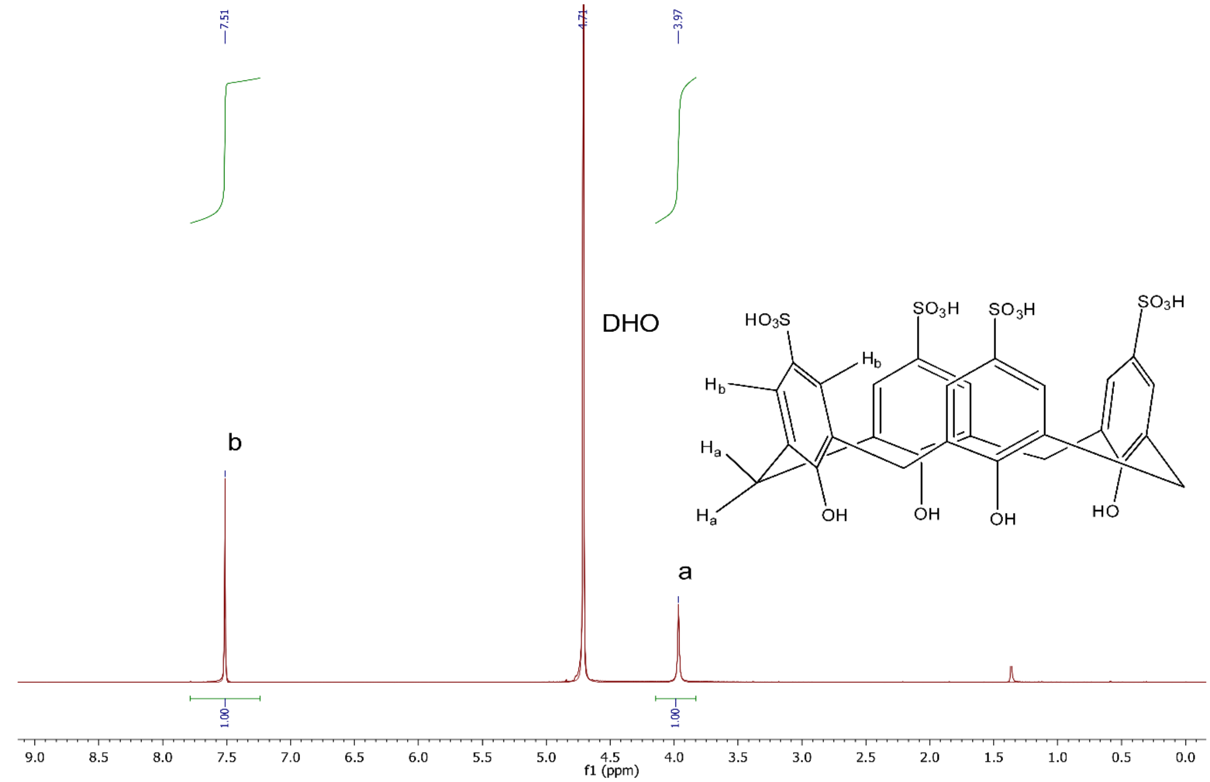

Figure S1. ^1H NMR spectrum of SCA in D_2O (300 MHz).

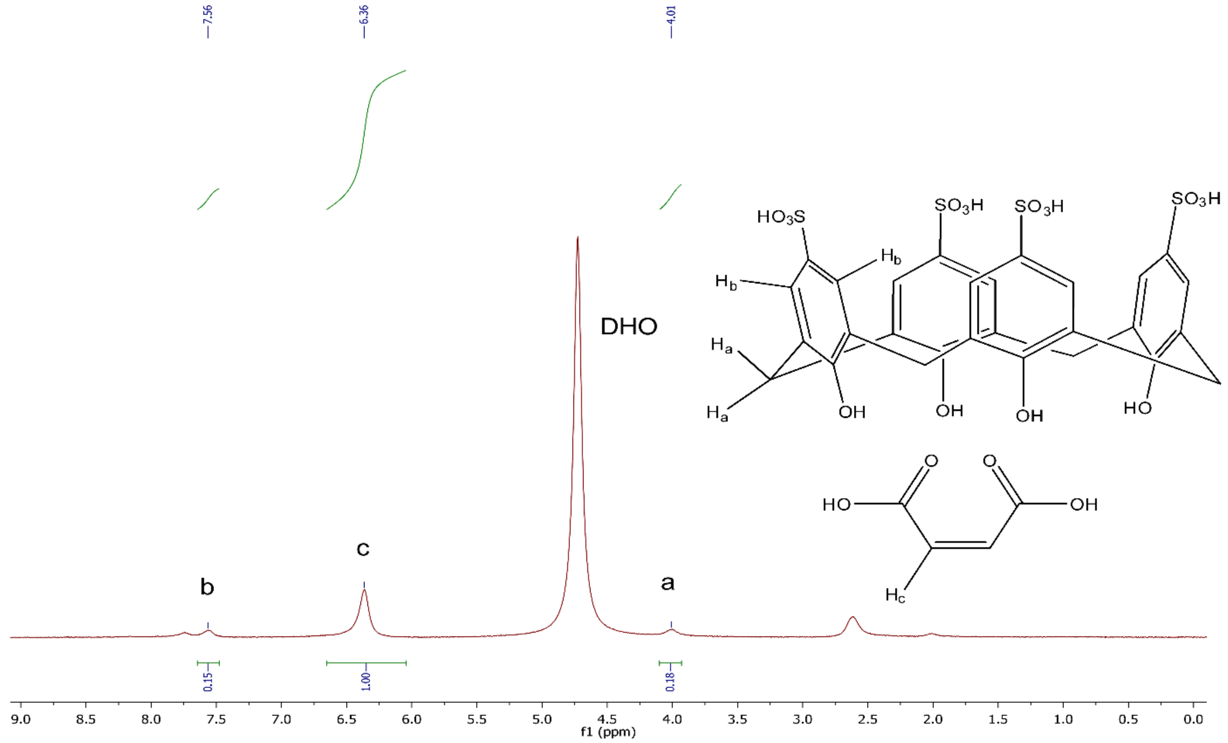

Figure S2. ^1H NMR spectrum of the supernatant solution after adsorptive loading of SCA@MIL-101-5 in D_2O (300 MHz). Maleic acid, MA (10 mg) was used as an internal standard.

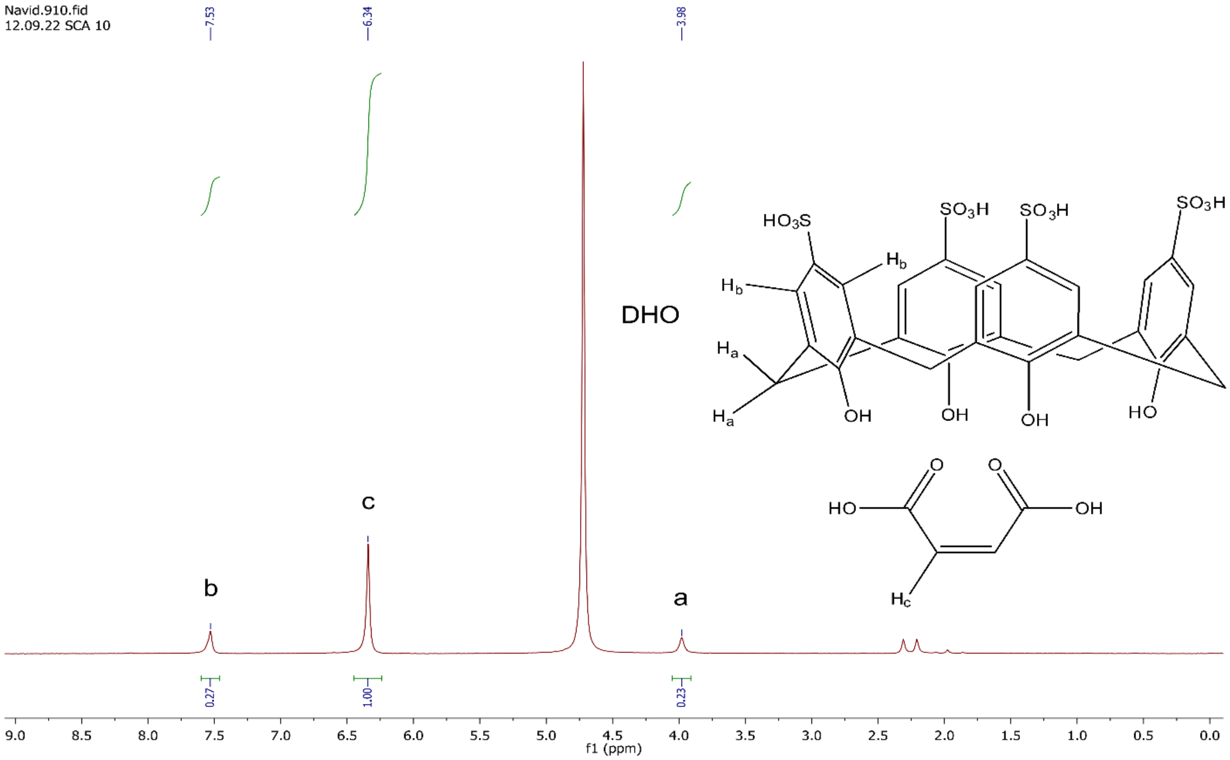

Figure S3. ^{1}H NMR spectrum of the supernatant solution after adsorptive loading of SCA@MIL-101-*10* in D_2O (300 MHz). Maleic acid, MA (10 mg) was used as an internal standard.

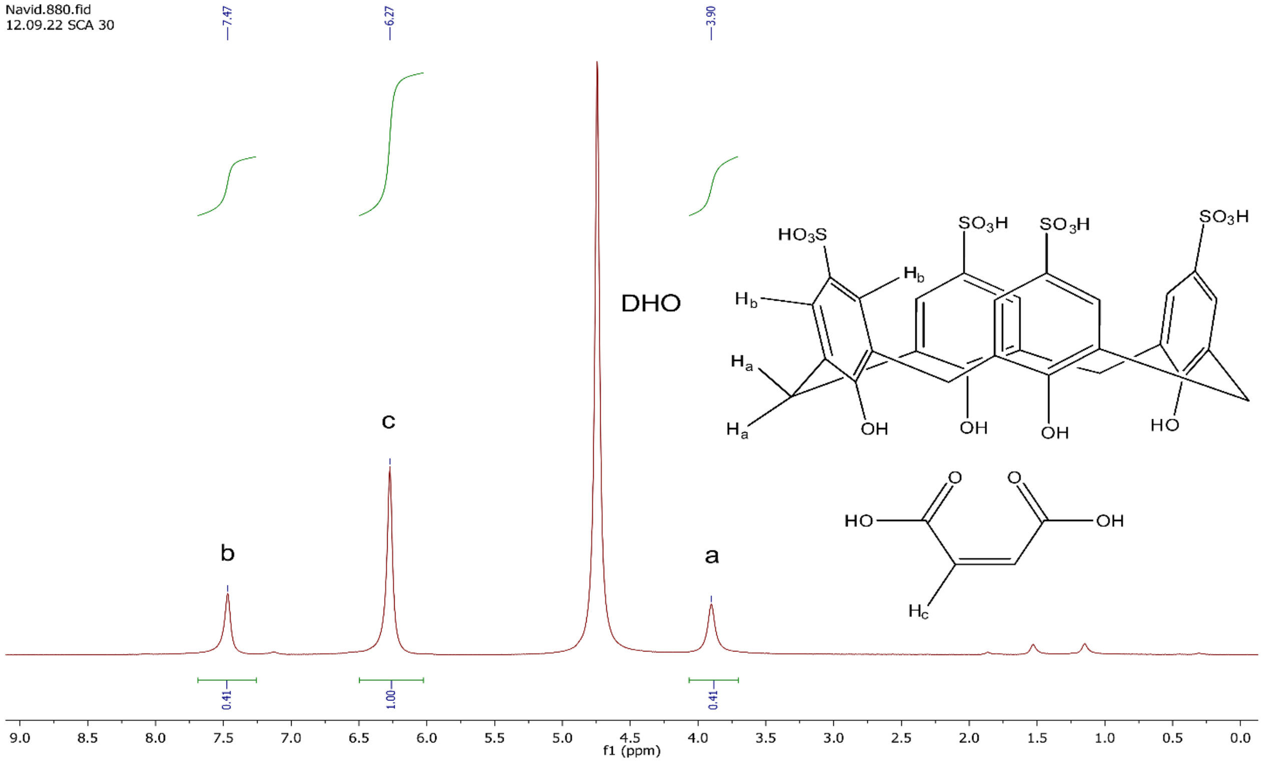

Figure S4. ^{1}H NMR spectrum of the supernatant solution after adsorptive loading of SCA@MIL-101-*30* in D_2O (300 MHz). Maleic acid, MA (10 mg) was used as an internal standard.

b) Digestion analysis of SCA@MIL-101-*30*:

The employed digestion method (using basic conditions), according to our knowledge, is the best one for a MIL-101 material, which is known for its high kinetic inertness.[5] 15 mg of the SCA@MIL-101-*30* composite was digested (i.e., the composite was decomposed, with the organic part being solubilized with a formation of a voluminous chromium hydroxide residue) in 0.5 mL of 2 mol/L of NaOH solution over 24 hours, including 30 min of sonication at the initial stage, to ensure complete digestion. Then, 2.0 mL of H_2O was added and the slurry was shaken for additional two days. The $Cr(OH)_3$ precipitate was removed by filtration through a plastic membrane (0.2 μm pore) to give a clear solution containing BDC^{2-} and SCA in deprotonated form under the alkaline conditions[4]. The solution was acidified by 1 mol/L HCl solution to pH = 3.0 with the formation of a H_2BDC precipitate, while the SCA remained in the solution due to sufficient solubility (5 g L^{-1} in water). The whole mixture was dried under a mild dynamic vacuum, first at 60 °C for 12 hours followed by drying at 90 °C for 6 hours. The residual powder was dispersed in 1.2 mL of D_2O and two drops of 40 wt% NaOD were added to give a clear solution for ^1H NMR analysis. The NaOD/D_2O solution was suitable for direct ^1H NMR quantification without water signal suppression, and contained the deprotonated SCA and BDC^{2-} species for relative ratio determination (Fig. S5). For the most SCA-rich composite, the SCA@MIL-101-*30*, 48 w% SCA content was established, which is held as a reasonably precise approximate of the maximal possible adsorptive capacity.

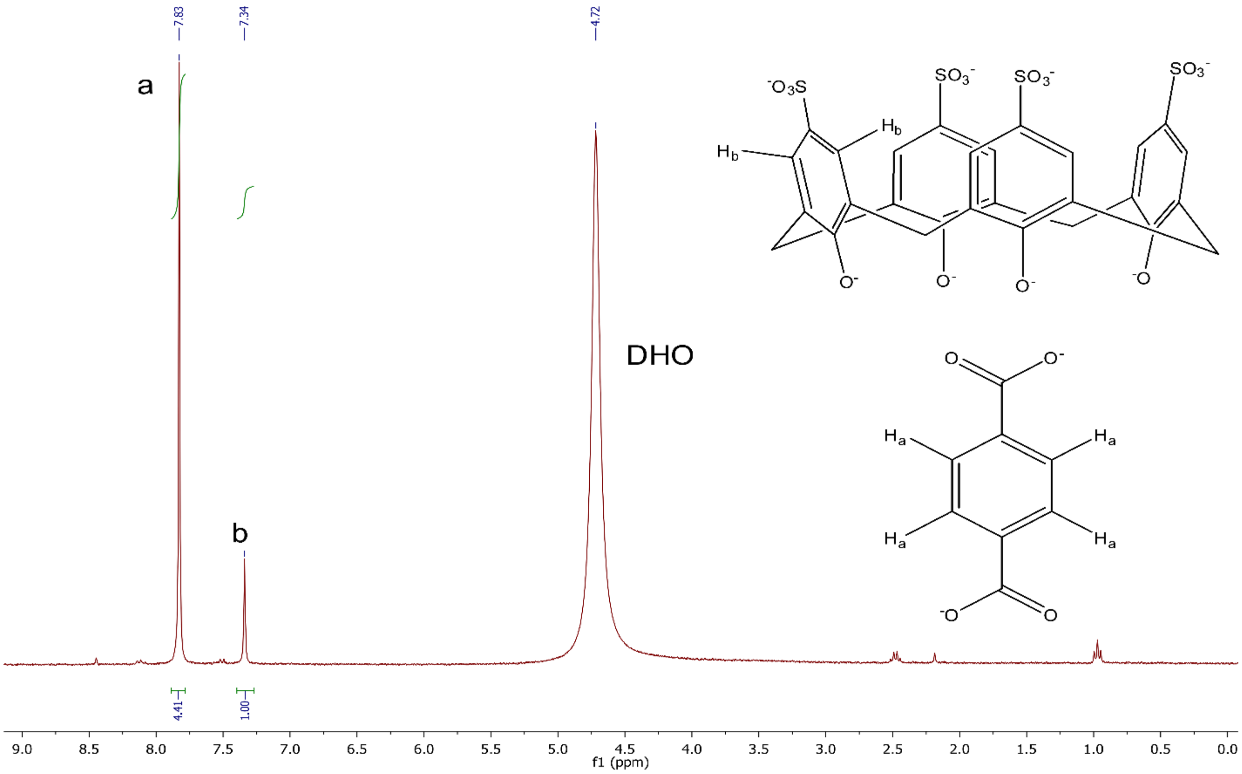

Figure S5. 1H NMR spectrum of digested SCA@MIL-101-30 in D2O/NaOD (300 MHz). The BDC2- ligand was used as an internal standard to calculate the SCA content in the composite.

Table S2 lists the SCA content in SCA@MIL-101-*30* based on the two NMR analyses.

Table S2. Comparison of SCA content for SCA@MIL-101-*30*.

Analysis	Molar ratio, x for SCA$_x$@MIL-101 a)	SCA weight content, %	Comment
NMR (digestion)	0.89	48	after the composite's digestion
NMR (supernatant)	0.96	50	analysis of supernatant after adsorptive loading

a) The MIL-101 host formula in the (SCA)$_x$@MIL-101 composite is assumed to be [$Cr_3O(H_2O)_2(BDC)_3$], i.e., with two terminal water molecule ligands (~5% weight difference compared to the dehydrated formula). Even though the samples for the analysis were activated, the terminal ligands are still accounted for the calculation; the latter is equivalent to accounting a partial rehydration during the transfer from vessel to vessel as well as minor residual impurities in the pores of the framework.

The CHNS elemental analysis provided an alternative estimation of the SCA content in the SCA@MIL-101 composites (Table S3). The differences between experimental and calculated values can be due to the possibility of water adsorption by composites.

Table S3. CHNS-based compositions of SCA@MIL-101.

Sample	%C	%H	%N	%S	Theoretical %S
MIL-101	41.32	2.56	1.04	0.12	0
SCA@MIL-101-*5*	38.85	2.72	0.27	1.62	3.77
SCA@MIL-101-*10*	39.47	2.78	0.31	3.05	4.78
SCA@MIL-101-*30*	40.21	2.84	0.33	5.35	5.88

3.5. SCA desorption tests on SCA@MIL-101 composite

To assess the desorption ("leaching") of the SCA from the composite SCA@MIL-101-*30* with the highest loading, 5 mg of the latter was dispersed in 1 mL of D_2O and heated at 60 °C overnight. After a final sonication for two minutes, the solution was filtered using a membrane filter (0.2 μm pore) to give a clear solution. The SCA content was determined by ^{1}H NMR analysis using maleic acid as an internal standard.

4. Figures

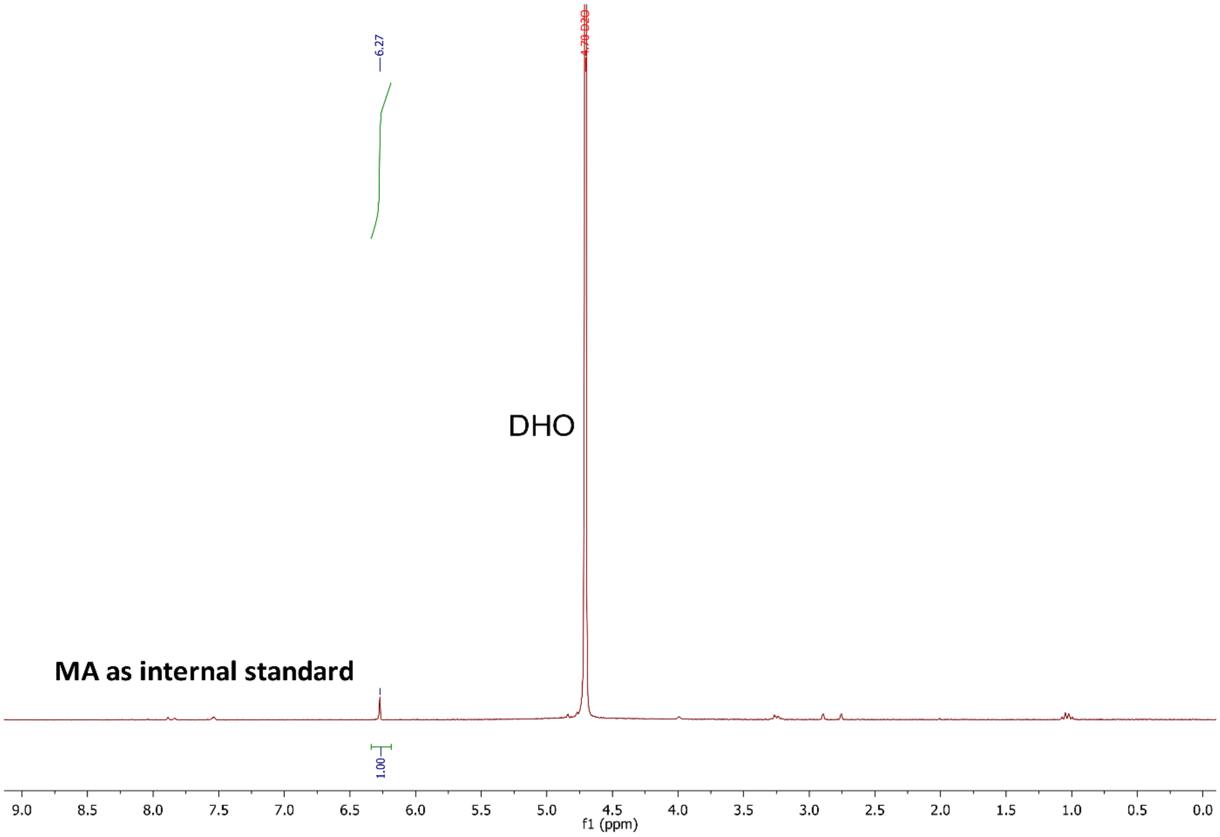

Figure S6. ^{1}H NMR spectrum of washed SCA@MIL-101-*30* with D_2O (300 MHz). Maleic acid, MA (10 mg) was used as an internal standard.

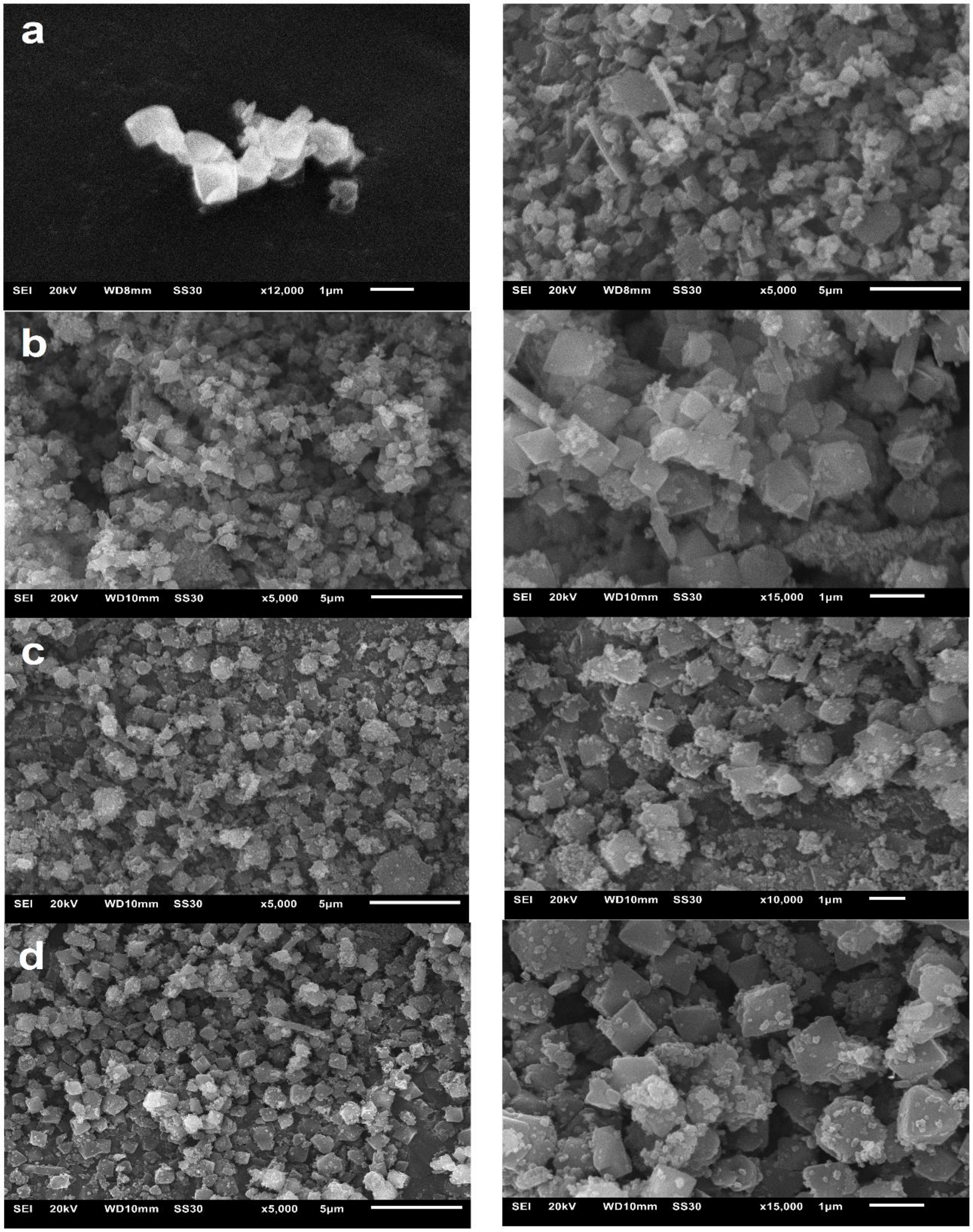

Figure S7. Representative SEM images of a) MIL-101, b) SCA@MIL-101-*5*, c) SCA@MIL-101-*10*, d) SCA@MIL-101-*30* (scale bar: 1 µm (left) and 5 µm (right)).

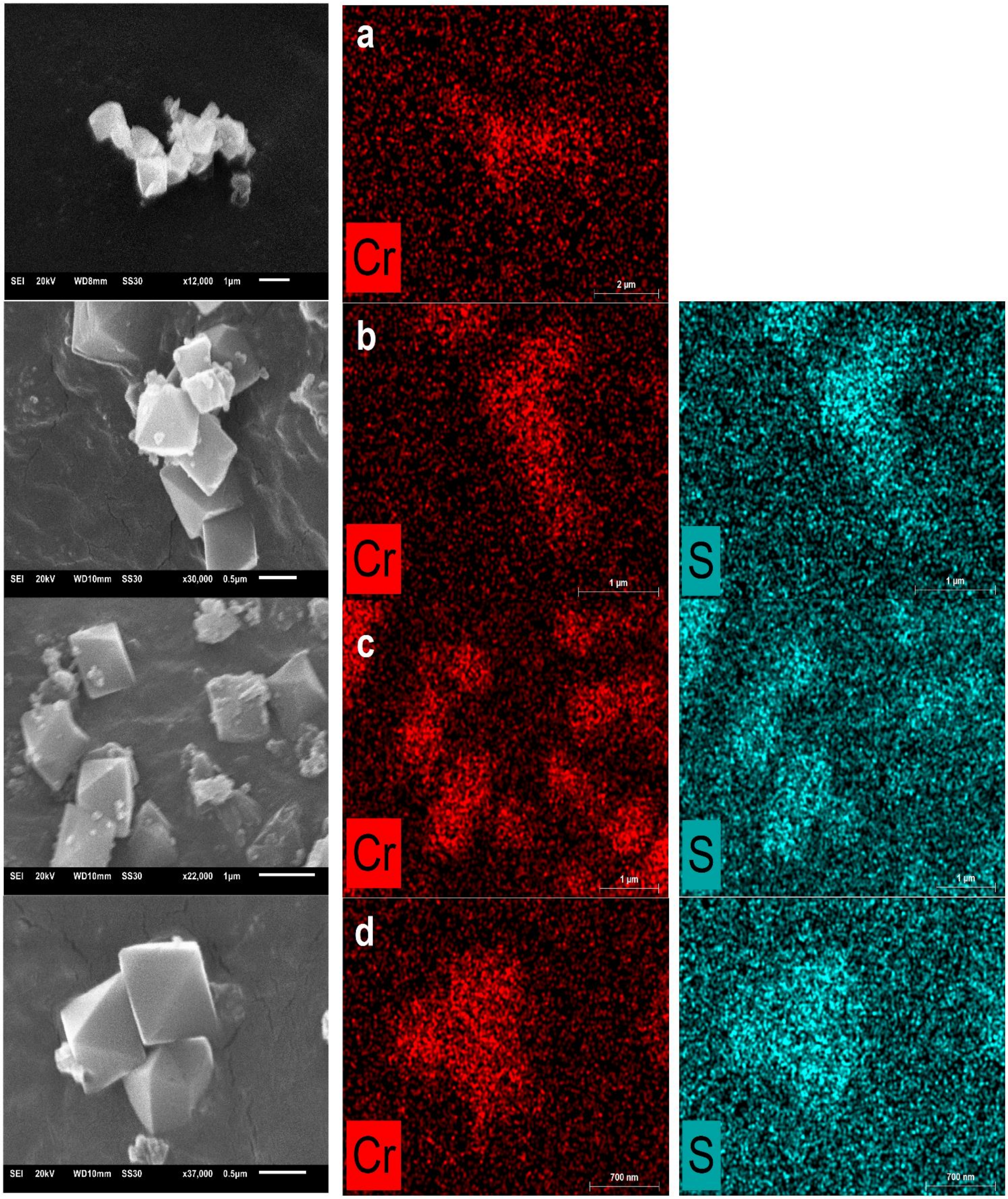

Figure S8. Representative MAPP images of a) MIL-101, b) SCA@MIL-101-*5*, c) SCA@MIL-101-*10*, d) SCA@MIL-101-*30*.

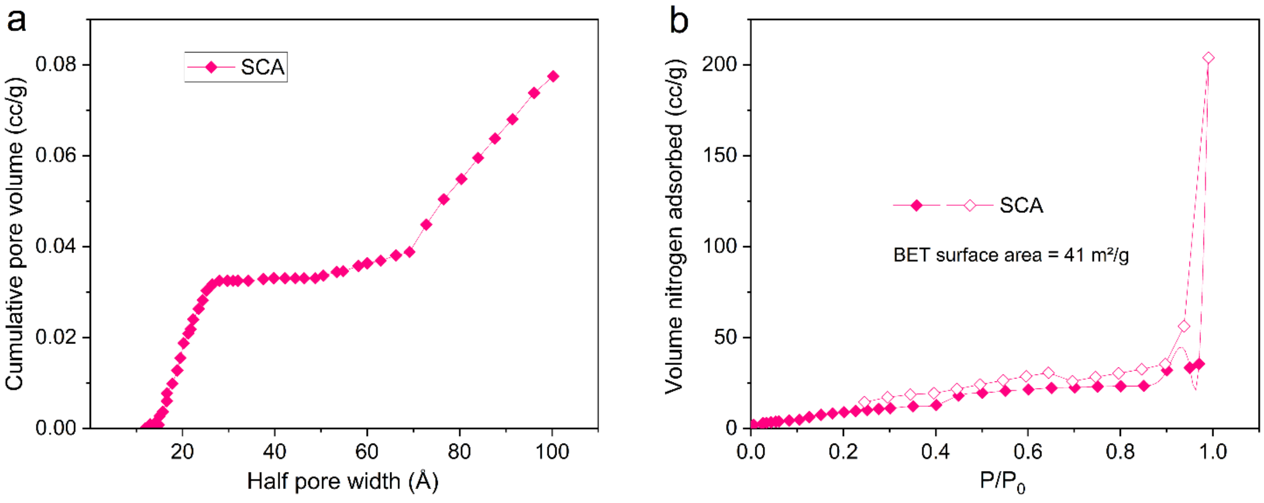

Figure S9. a) N_2 sorption isotherms at 77 K, and b) cumulative pore volume of SCA supramolecular cage. Filled and empty symbols represent adsorption and desorption, respectively.

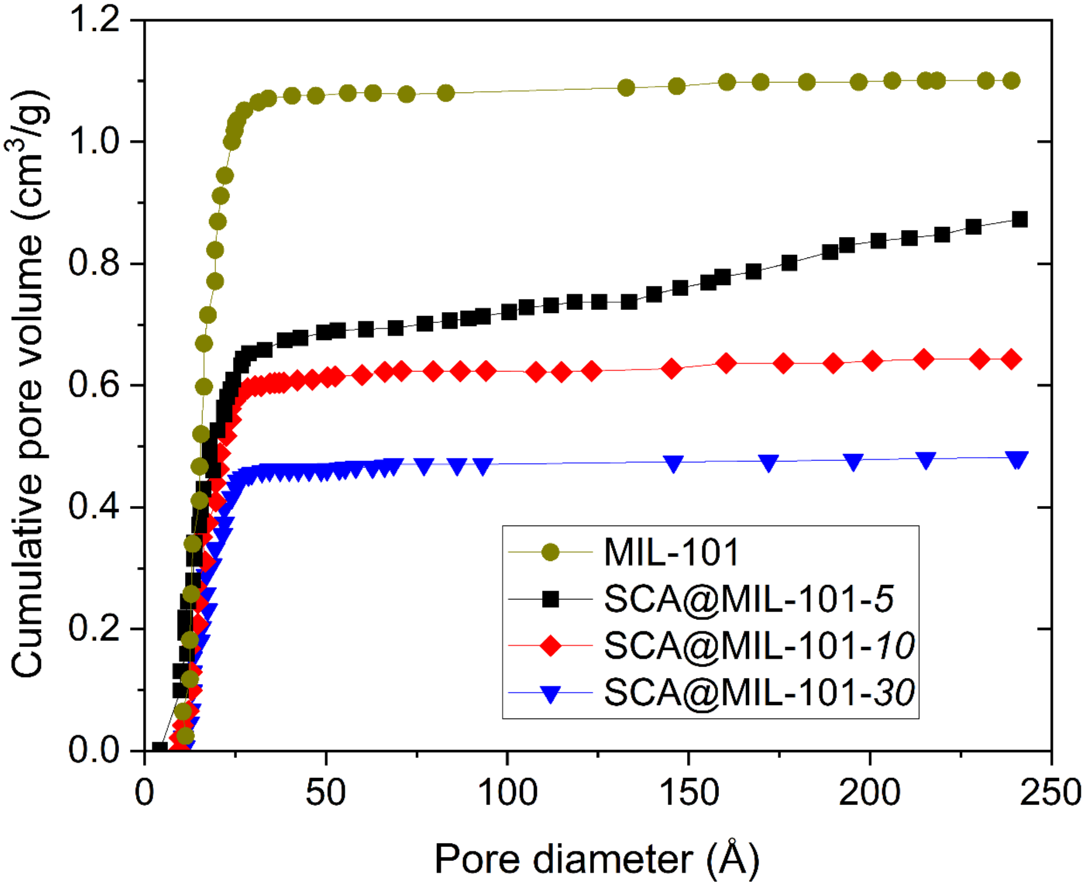

Figure S10. Cumulative pore volume of MIL-101 and all composites.

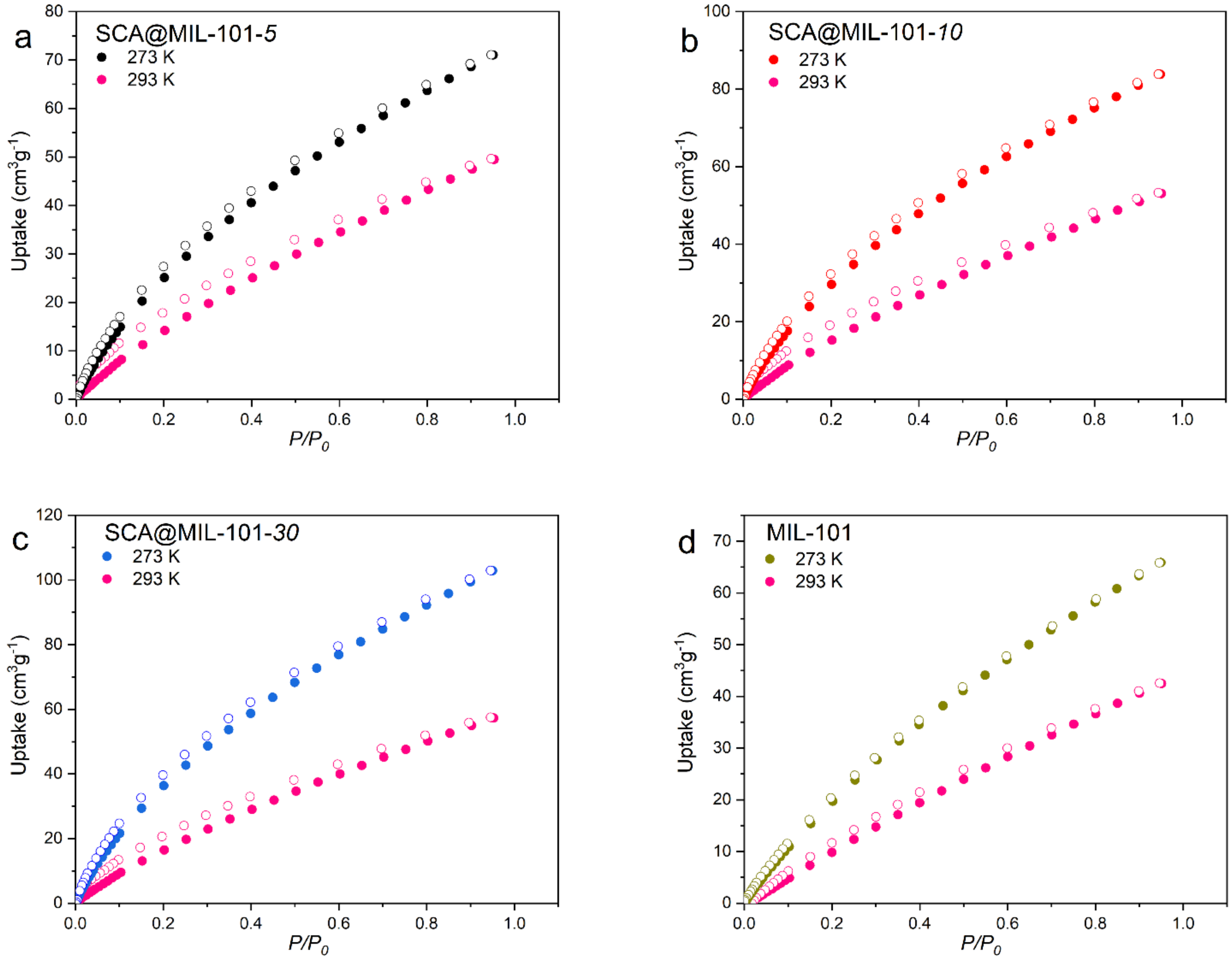

Figure S11. CO_2 sorption isotherms of a) SCA@MIL-101-*5*, b) SCA@MIL-101-*10*, c) SCA@MIL-101-*30*, and d) MIL-101 measured up to 1 bar at 273 K and 293 K, respectively. Filled and empty symbols represent adsorption and desorption, respectively.

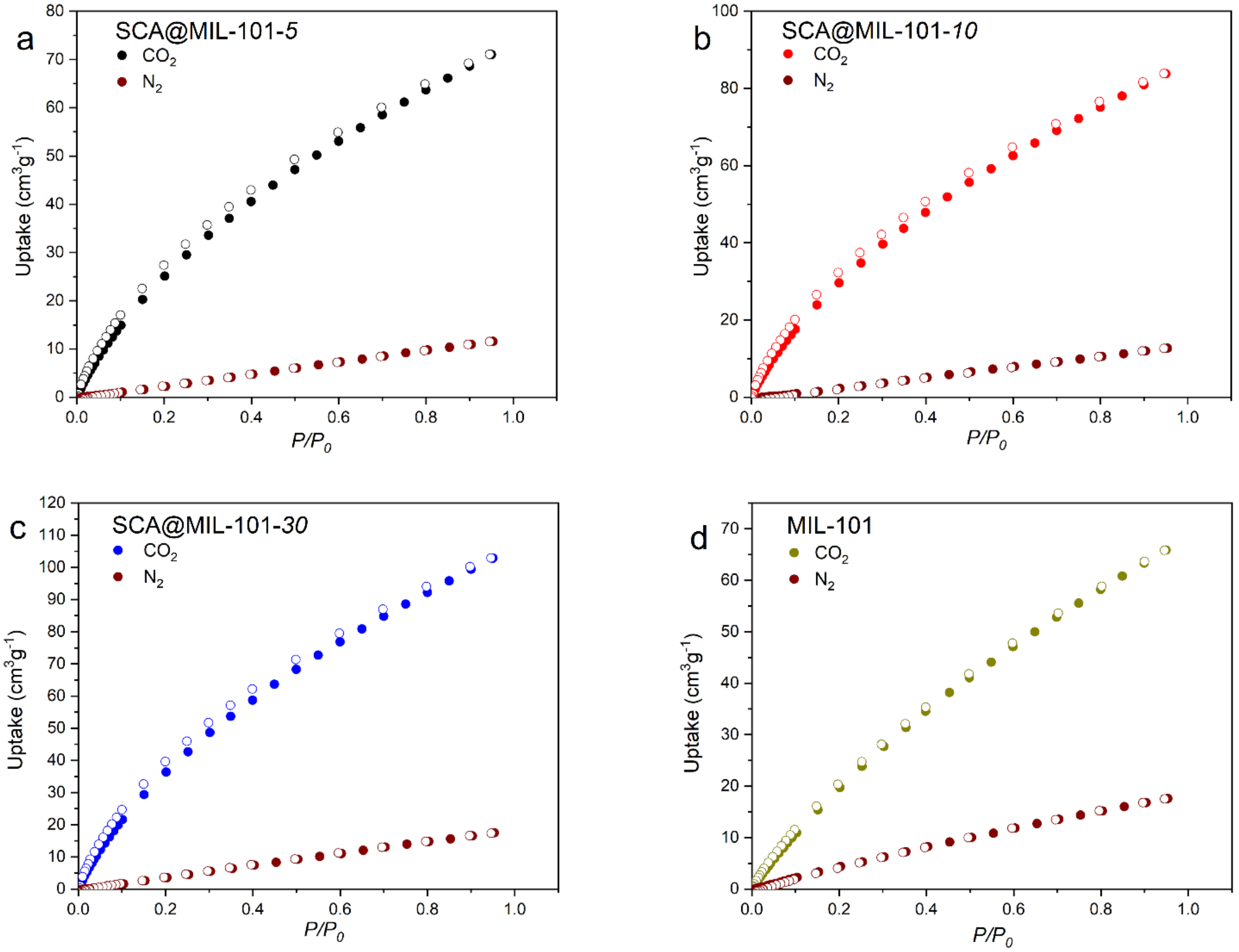

Figure S12. CO_2 and N_2 sorption isotherms of a) SCA@MIL-101-*5*, b) SCA@MIL-101-*10*, c) SCA@MIL-101-*30*, and d) MIL-101 measured up to 1 bar at 273 K. Filled and empty symbols represent adsorption and desorption, respectively.

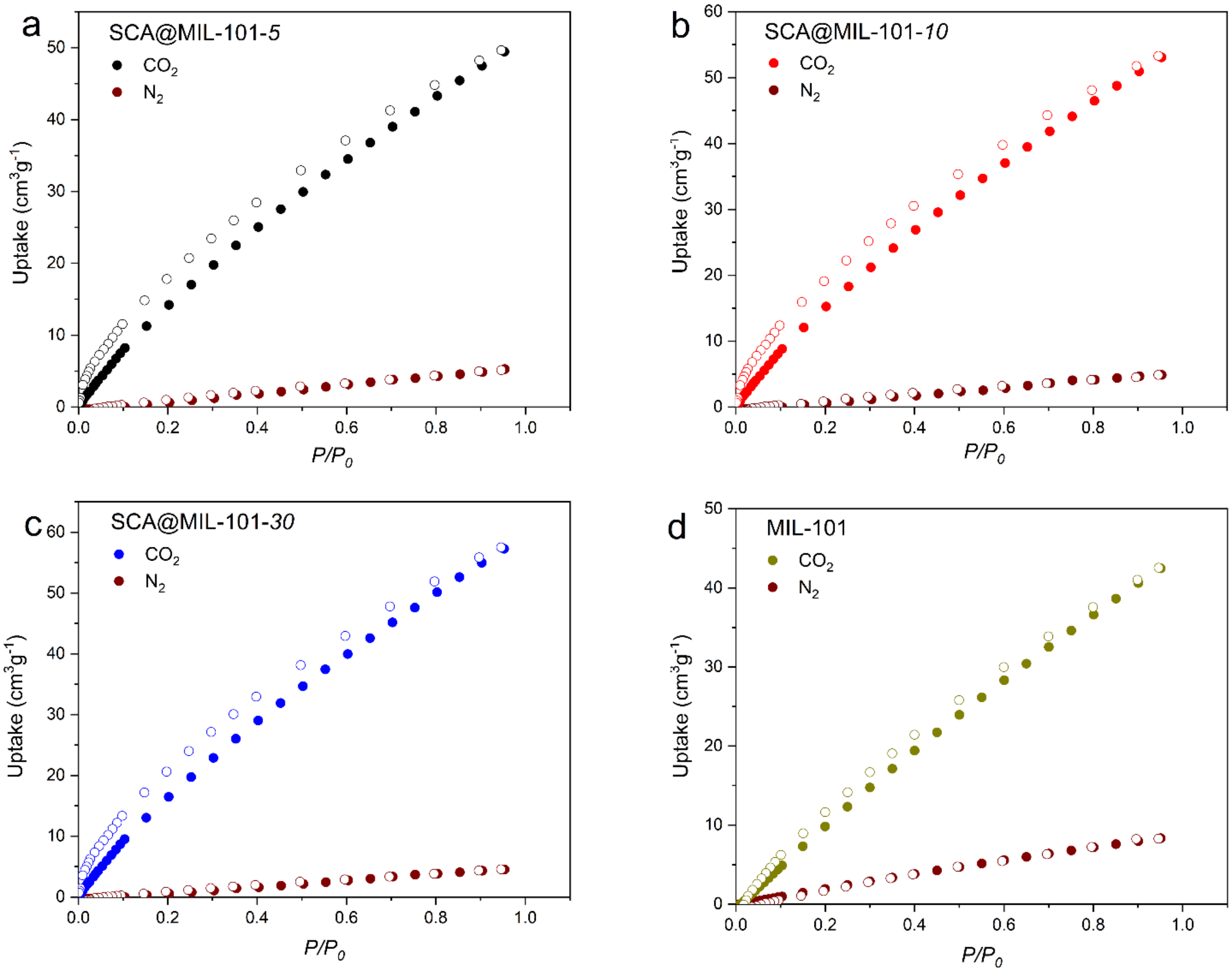

Figure S13. CO$_2$ and N$_2$ sorption isotherms of a) SCA@MIL-101-*5*, b) SCA@MIL-101-*10*, c) SCA@MIL-101-*30*, and d) MIL-101 measured up to 1 bar at 293 K. Filled and empty symbols represent adsorption and desorption, respectively.

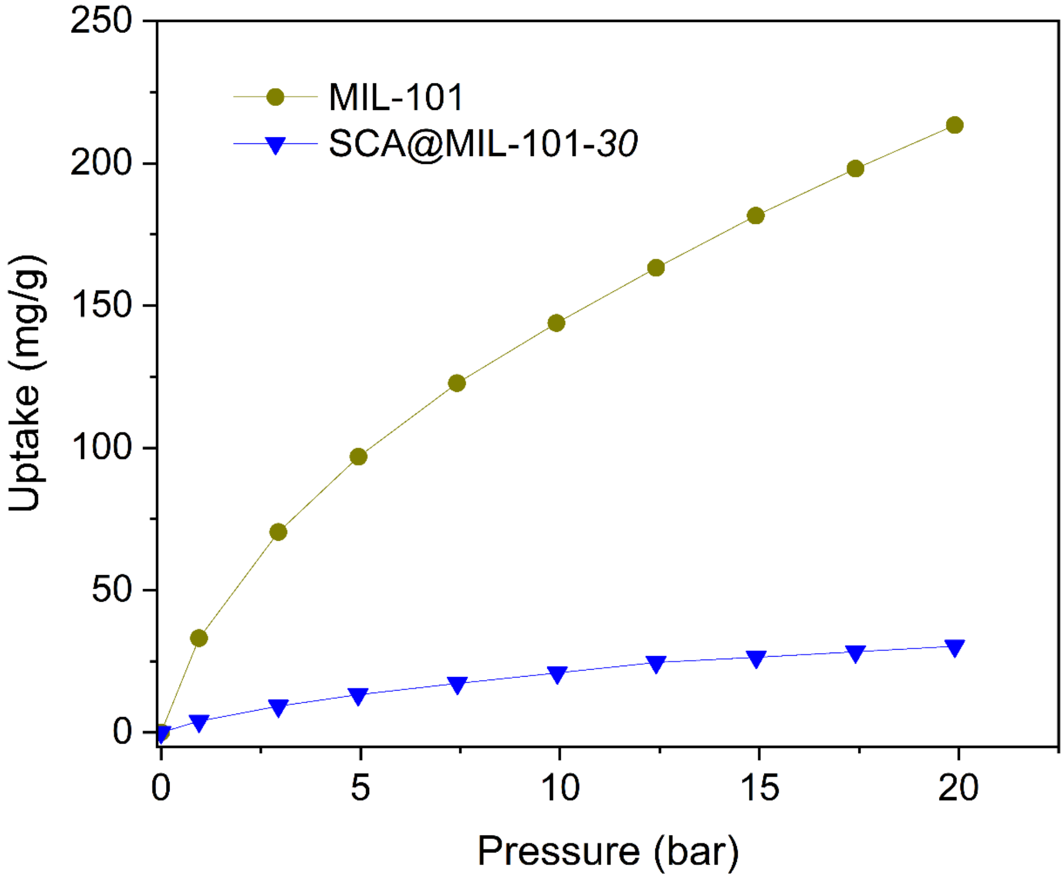

Figure S14. CO_2 adsorption isotherms of MIL-101 and SCA@MIL-101-*30* up to 20 bar at 293 K.

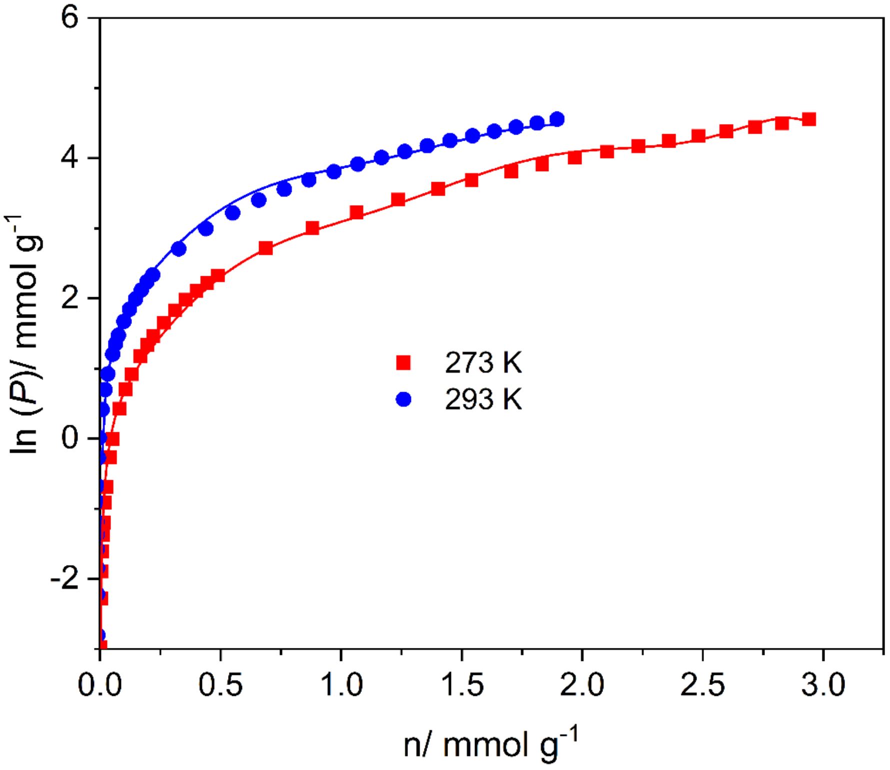

Figure S15. Virial analysis of the CO_2 sorption data for MIL-101. a_0 = -4463.92427, a_1 = -155.06748, a_2 = 6345.26677, a_3 = -10828.707, a_4 = 9514.43327, b_0 = 19.70111, b_1 = -5.29558. n= 0.01 was chosen as the lowest common data point.

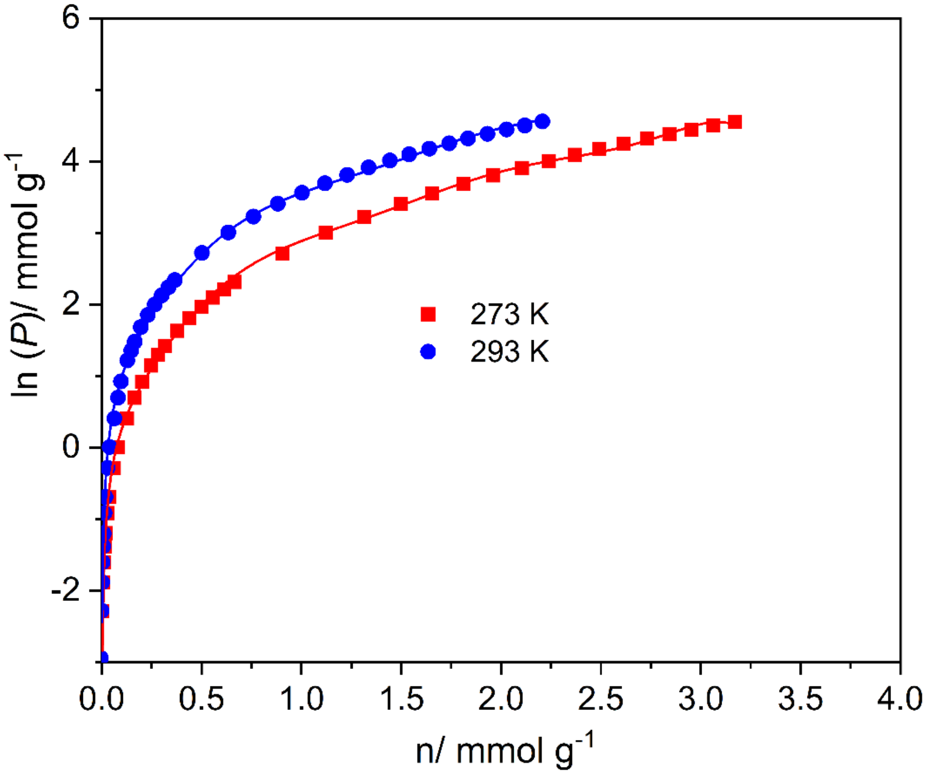

Figure S16. Virial analysis of the CO_2 sorption data for SCA@MIL-101-5. a_0 = -2879.39973, a_1 = -947.03918, a_2 = 4452.18956, a_3 = -6939.79129, a_4 = 5500.13207, b_0 = 13.38185, b_1 = -0.66197. n= 0.01 was chosen as the lowest common data point.

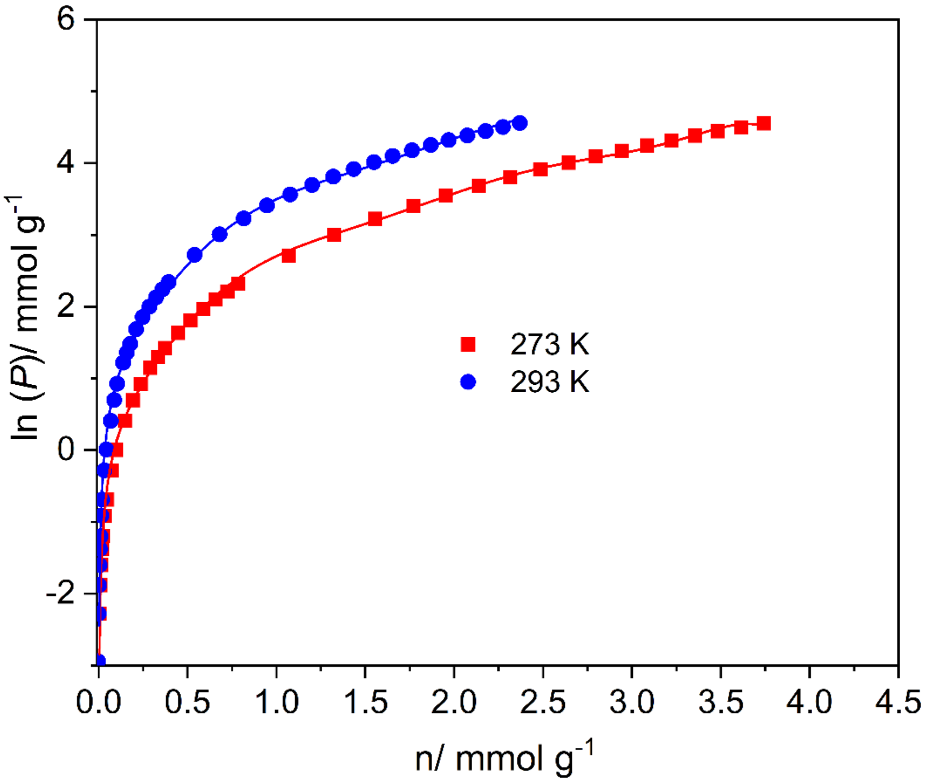

Figure S17. Virial analysis of the CO_2 sorption data for SCA@MIL-101-*10*. a_0 = -3236.82556, a_1 = -877.58407, a_2 = 3115.3435, a_3 = -4092.3733, a_4 = 2729.94979, b_0 = 14.52192, b_1 = -0.20453. n= 0.01 was chosen as the lowest common data point.

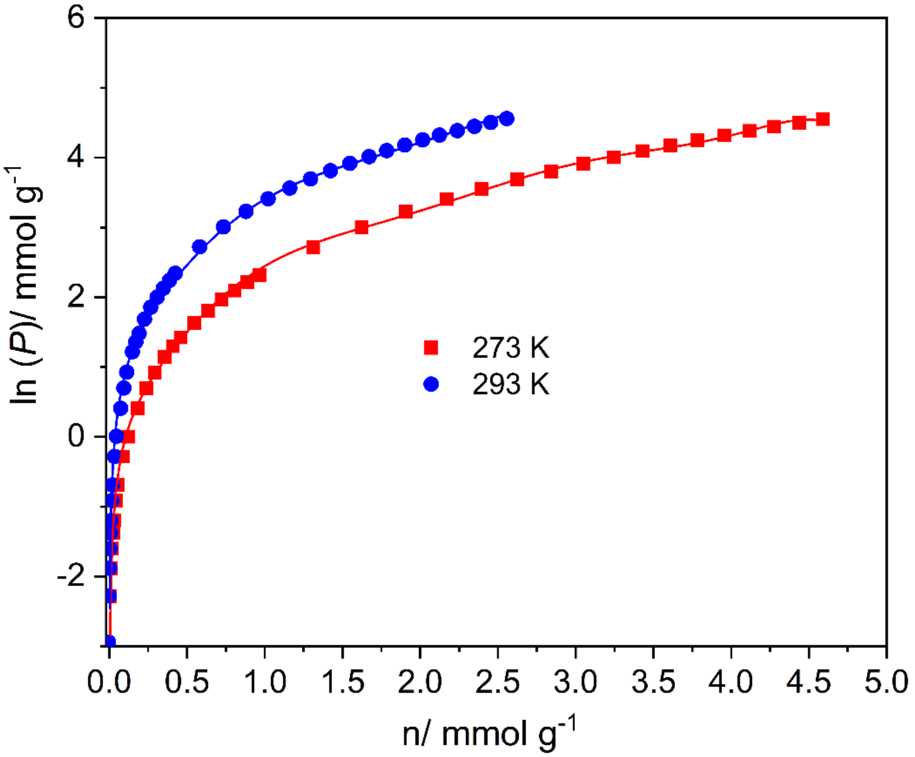

Figure S18. Virial analysis of the CO_2 sorption data for SCA@MIL-101-*30*. a_0 = -3910.28402, a_1 = -406.03218, a_2 = 2076.16222, a_3 = -2255.55125, a_4 = 1232.40056, b_0 = 16.05004, b_1 = 0.39804. n= 0.01 was chosen as the lowest common data point.

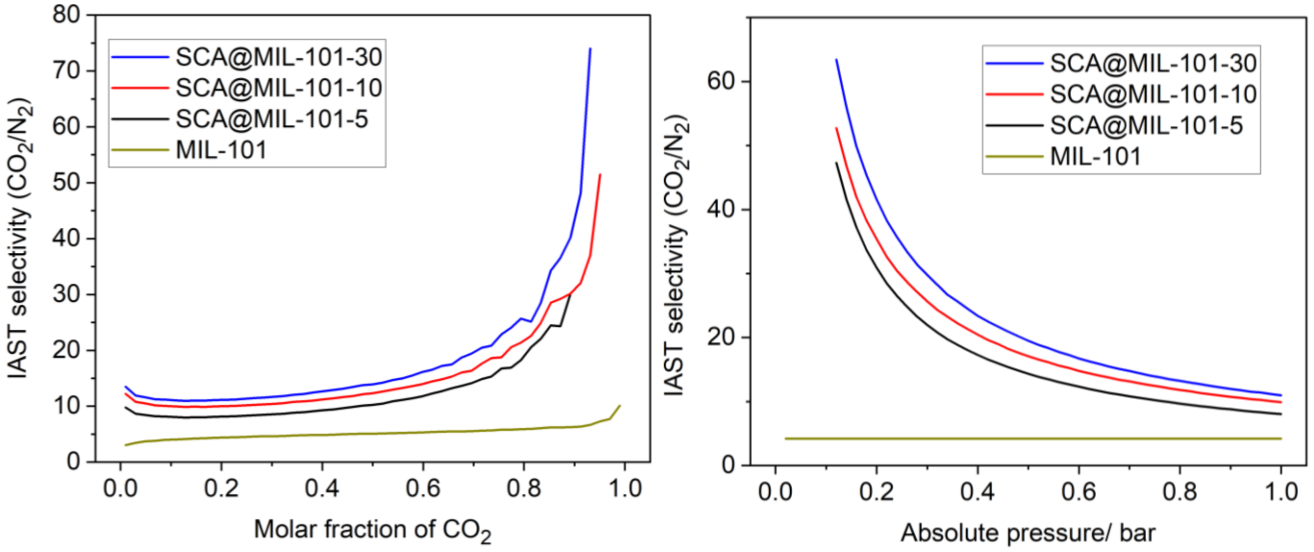

a) b)

Figure S19. a) CO_2/N_2 selectivity as a function of molar CO_2 fraction of MIL-101, SCA@MIL-101-*5*, SCA@MIL-101-*10*, and SCA@MIL-101-*30* calculated by IAST technique at 293 K and 1 bar. The strong increase in selectivity above a molar CO_2 fraction of 0.8 (N_2 0.2) is caused by the adsorbed nitrogen amount getting closer to zero at low partial pressure. b) CO_2/N_2 selectivity as a function of absolute pressure for a 15:85 v:v CO_2/N_2 gas mixture.

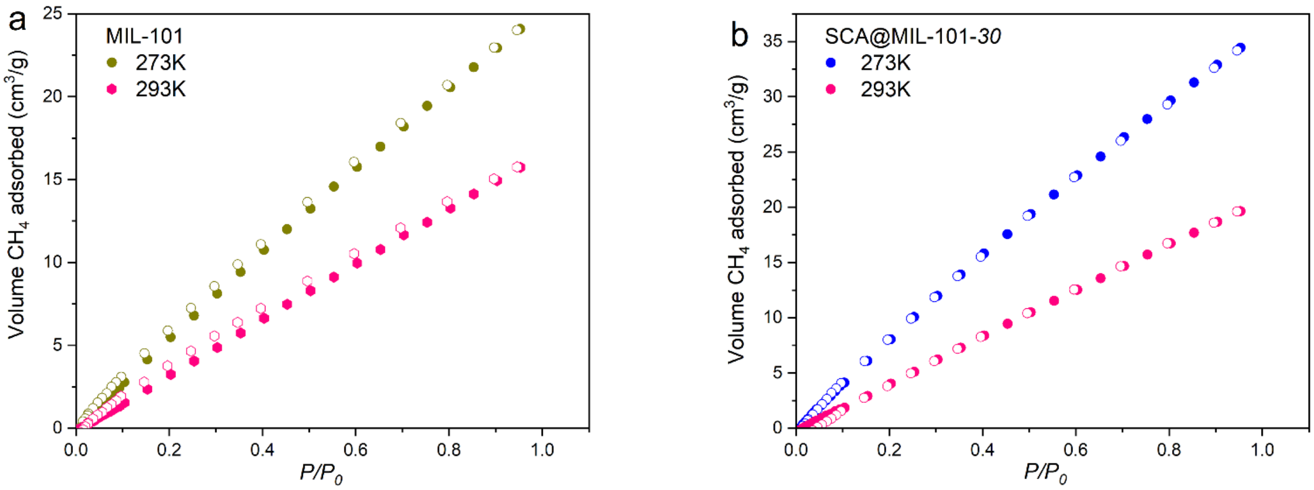

Figure S20. CH_4 sorption isotherms of a) MIL-101 and b) SCA@MIL-101-*30*, measured up to 1 bar at 273 K and 293K, respectively. Filled and empty symbols represent adsorption and desorption, respectively.

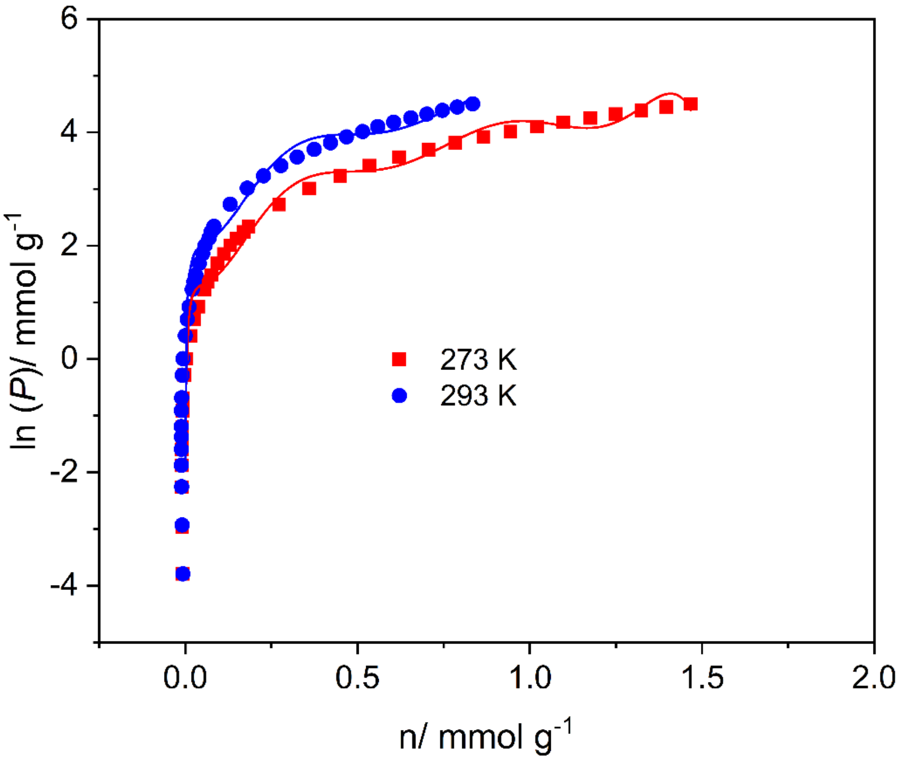

Figure S21. Virial analysis of the CH_4 sorption data for MIL-101. a_0 = -1657.73565, a_1 = -7808.29252, a_2 = 79182.87917, a_3 = -364264.67131, a_4 = 874976.63155, b_0 = 11.50705, b_1 = -0.52851. n= 0.001 was chosen as the lowest common data point.

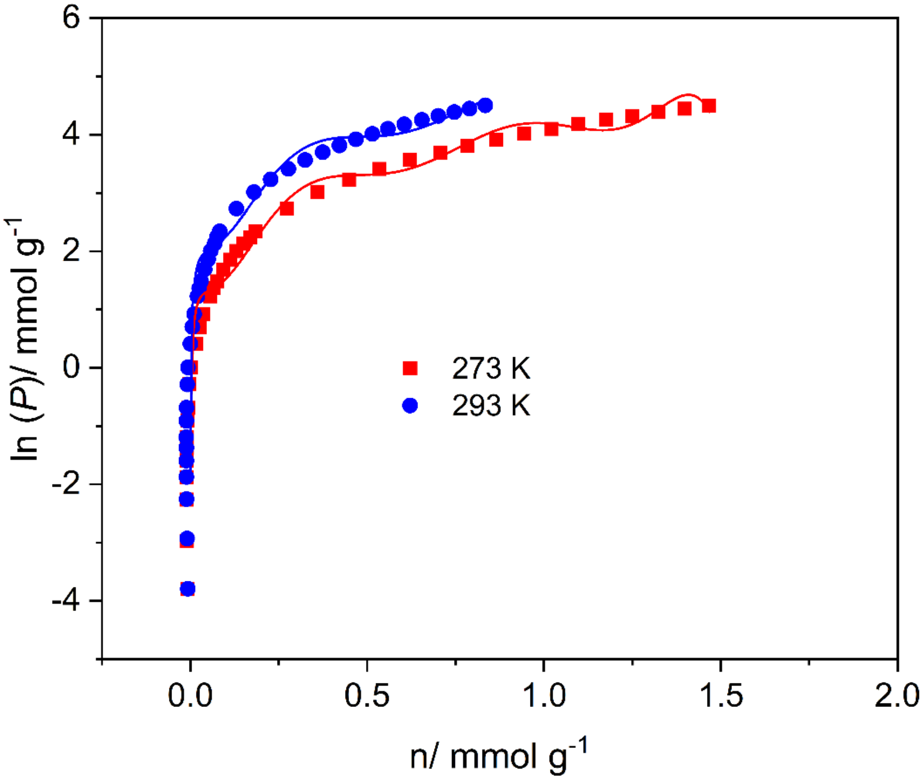

Figure S22. Virial analysis of the CH_4 sorption data for SCA@MIL-101-*30*. a_0 = -2453.62671, a_1 = -10503.98429, a_2 = 83598.98868, a_3 = -280365.16151, a_4 = 483066.76908, b_0 = 14.68825, b_1 = -2.23107. n= 0.001 was chosen as the lowest common data point.

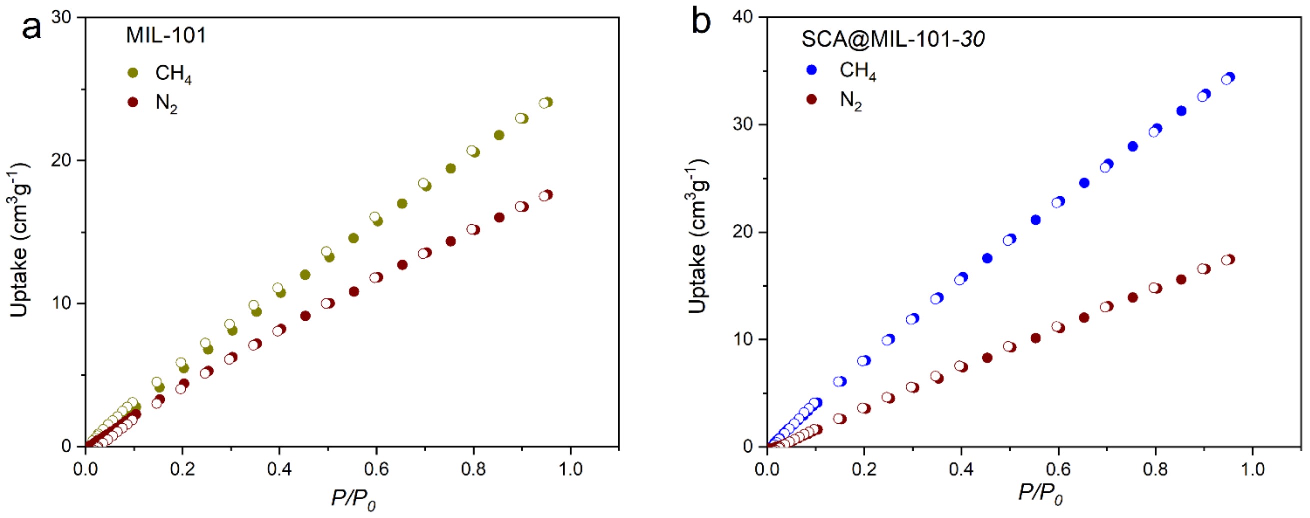

Figure S23. CH_4 and N_2 sorption isotherms of a) MIL-101 and b) SCA@MIL-101-*30*, measured up to 1 bar at 273 K, respectively. Filled and empty symbols represent adsorption and desorption, respectively.

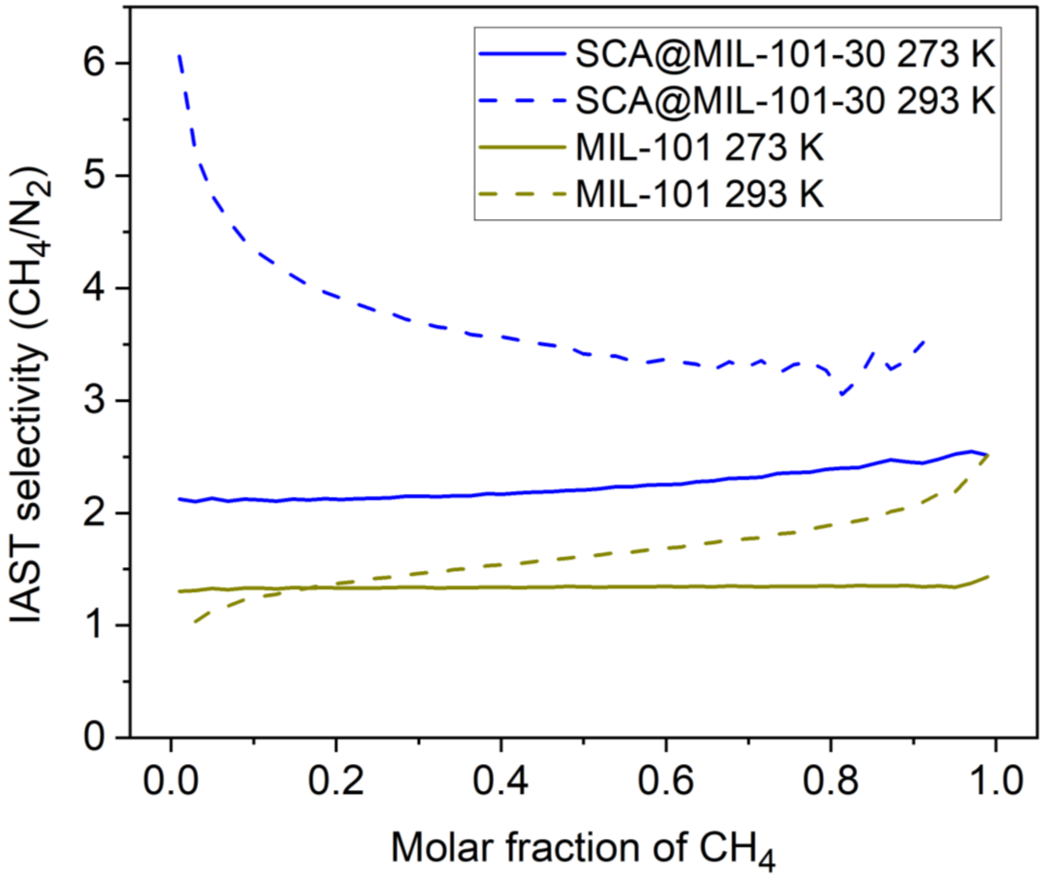

Figure S24. CH_4/N_2 selectivity of MIL-101 and SCA@MIL-101-*30* calculated by IAST for a gas mixture of CH_4/N_2 at 273 K and 293 K at 1 bar.

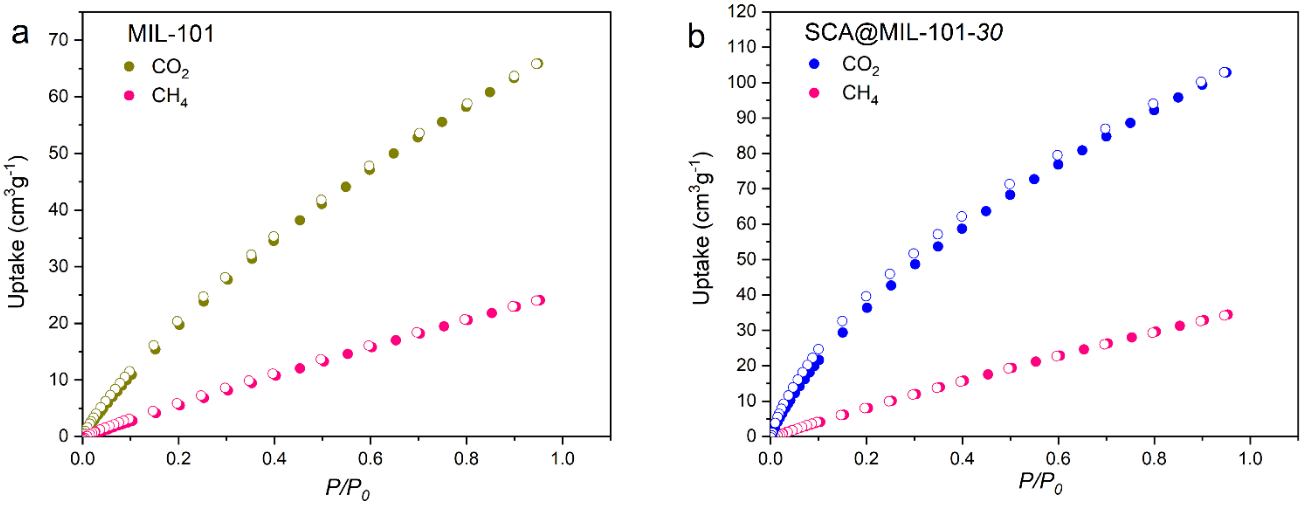

Figure S25. CO_2 and CH_4 sorption isotherms of a) MIL-101 and b) SCA@MIL-101-*30*, measured up to 1 bar at 273 K, respectively. Filled and empty symbols represent adsorption and desorption, respectively.

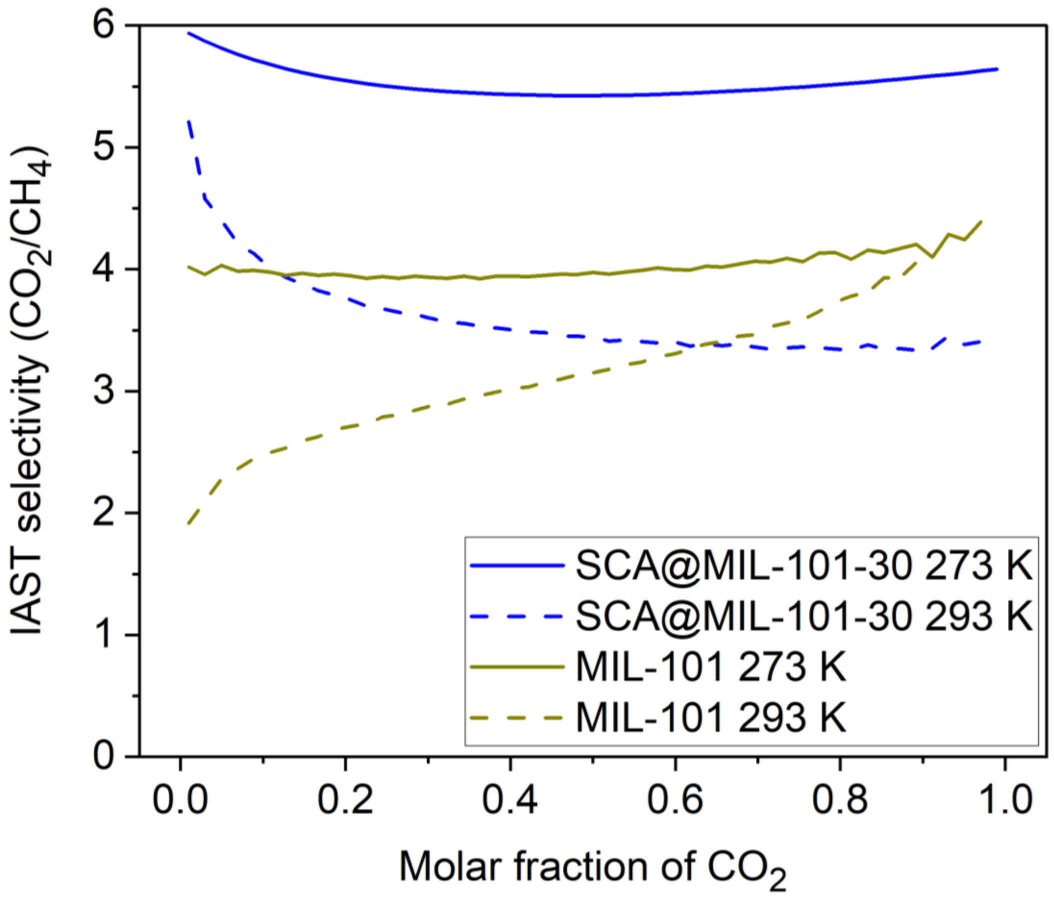

Figure S26. CO_2/CH_4 selectivity of MIL-101 and SCA@MIL-101-*30* calculated by IAST for a gas mixture of CO_2/CH_4 at 273 K and 293 K at 1 bar.

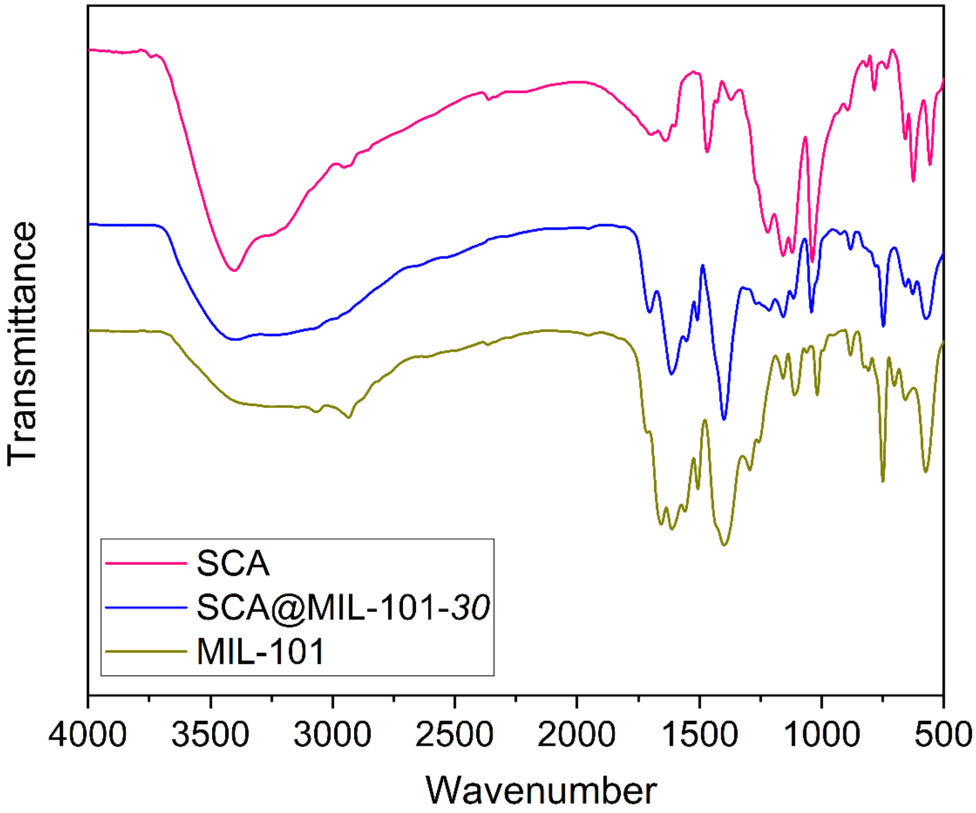

Figure S27. FT-IR spectra of SCA, MIL-101 and SCA@MIL-101-*30*.

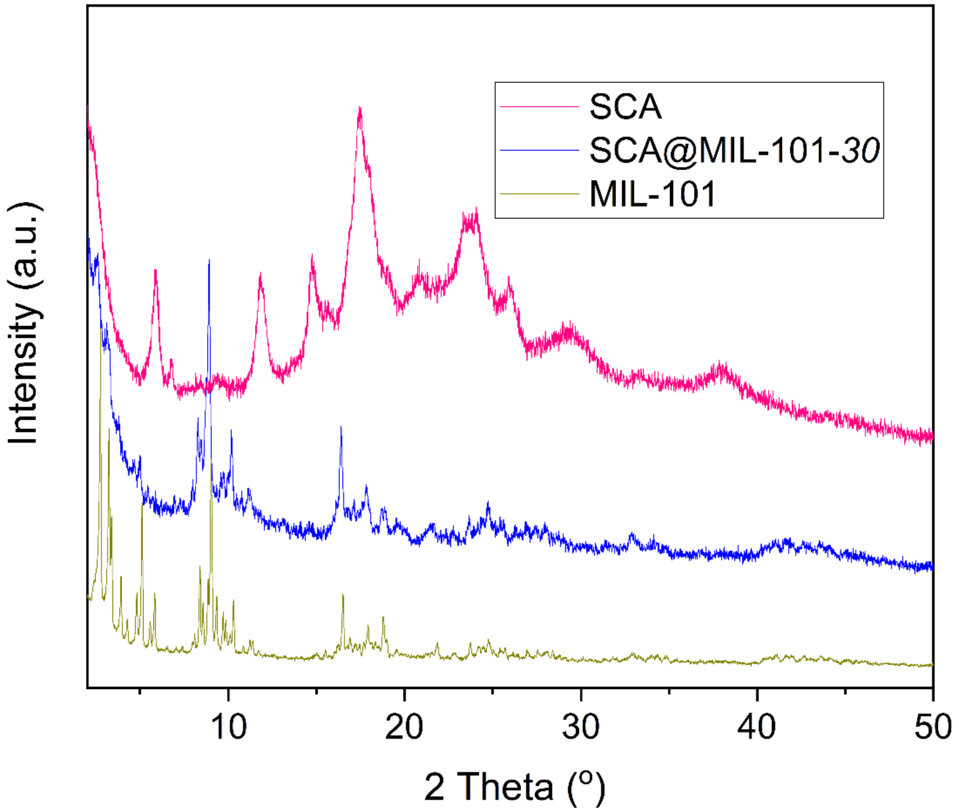

Figure S28. PXRD patterns of SCA, MIL-101, and SCA@MIL-101-*30*.

Figure S29. Aluminum block for catalytic simultaneous esterification reactions.

5. Tables S4 to S6

Table S4 CO_2 uptake for MIL-101 and SCA@MIL-101 composites at 273 K and 293 K.

Sample	mmol/g	Wt% [a)]	T (K)
MIL-101	1.9	8	293
	2.9	11	273
SCA@MIL-101-*5*	2.2	9	293
	3.2	12	273
SCA@MIL-101-*10*	2.4	9.5	293
	3.7	14	273
SCA@MIL-101-*30*	2.6	10	293
	4.6	17	273

a) Wt% was calculated from the uptake X in mmol according to:

$X \times 0.044$ g/mmol = Y [g] and

$Y / (Y + 1) \times 100\% = \mathrm{Wt\%}$

Table S5 CO_2, N_2 and CH_4 uptakes at 1 bar, selectivities, isosteric heats of adsorptions and BET surface areas of SCA, MIL-101, and SCA@MIL-101-*w* (*w* = *5*, *10*, *30*) composites.

sample	BET (m^2 g^{-1})	Total pore volume (cm^3 g^{-1})	CO_2 uptake (cm^3 g^{-1})	N_2 uptake (cm^3 g^{-1})	CH_4 uptake (cm^3 g^{-1})	**T (K)**	Selectivity CO_2/N_2 (15:85) at 1 bar	Selectivity CO_2/CH_4 (25:75) at 1 bar	Selectivity CH_4/N_2 (15:85) at 1 bar	Q_{st}^0 for CH_4 kJ mol^{-1}	Q_{st}^0 for CO_2 kJ mol^{-1}
SCA	41	0.079									
MIL-101	2658 a)	0.996	42.46	8.2	15.8	**293**	4	3	1	22	48
			65.8	17.6	24.1	**273**	5	4	1		
SCA@MIL-101-*5*	2156	0.790	49.44	5.2	---	**293**	8	---	---		33
			71.0	11.5	---	**273**	9.5	---	---		
SCA@MIL-101-*10*	1497 b)	0.650	53.06	4.8	---	**293**	10	---	---		37
			83.8	12.6	---	**273**	9	---	---		
SCA@MIL-101-*30*	1073 c)	0.519	57.5	4.5	19.7	**293**	11	4	4	31	42
			102.9	17.4	34.2	**273**	9	~6	2		

a) C constant: 63.2, R^2: 0.999145, b) C constant: 150.8, R^2: 0.999891, c) C constant: 128.8, R^2: 0.999857.

Table S6 Lower-pressure CO_2 adsorption capacities for MIL-101 and selected functional composites at 273-319 K.

Common name a)	BET surface area (m^2 g^{-1})	CO_2 capacity (Wt %) b)	Pressure (bar)	Temperature (K)	Reference
MWCNT@MIL-101	---	0.33	1	298	6
MWCNT@MIL-101	1243	5.93	10	298	7
1.3 wt.% RHA-MIL-101(Cr)	3333	4.66	1	298	8
MAX-MIL	2670	7.20	10	300	9
2 wt.% MWCNT/MIL-101	3146	15.40	1	298	10
MIL-101	3745	13.20	1	298	10
NH_2–Cr–MIL-101	1675	12.32	1	298	11
TAEA@MIL-101	1279	9.63	1	298	12
ED@MIL-101	1585	8.49	1	298	12
TEDA@MIL-101	1807	7.26	1	298	12
MIL-101	3483	7.08	1	298	12
MIL-101	1870	9.25	1	298	13
MIL-101/PPD	1007	7.48	1	298	14
DMEDA-MIL-101	1018	7.03	1	298	15
MIL-101	2132	5.94	1	298	15
MIL-101	2674	4.20	1	319	16
MIL-101	2658	7.1	1	293	This work
SCA@MIL-101-*5*	2156	8.1	1	293	This work
SCA@MIL-101-*10*	1497	8.6	1	293	This work
SCA@MIL-101-*30*	1073	9.5	1	293	This work
MIL-101	2658	10	1	273	This work
SCA@MIL-101-*5*	2156	12	1	273	This work
SCA@MIL-101-*10*	1497	14	1	273	This work

SCA@MIL-101-*30*	1073	17	1	273	This work

MWCNT: Multi-walleded carbon nanotubes, RHA: Silica-rich rice husk ash, MAX: Activated carbon powder, TEPA: Tetraethylenepentamine; TAEA: Tris(2-aminoethyl) amine, ED: Ethylenediamine, TEDA: Triethylenediamine, PPD: Phenylenediamine, DMEDA: *N,N'*-dimethylethylenediamine.

[b)] Calculated based on the given uptake capacity in corresponding references.

5. References

1 Y. Tauran, A. Brioude, P. Shahgaldian, A. Cumbo, B. Kim, F. Perret, A. W. Coleman and I. Montasser, *Chem. Commun.*, 2012, **48**, 9483-9485. DOI: 10.1039/C2CC34670B

2 T. Zhao, F. Jeremias, I. Boldog, B. Nguyen, S. K. Henninger and C. Janiak, *Dalton Trans.*, 2015, **44**, 16791-16801. DOI: 10.1039/C5DT02625C

3. Y. Dou, H. Zhang, A. Zhou, F. Yang, L. Shu, Y. She and J. R. Li, *Ind. Eng. Chem. Res.*, 2018, **57**, 8388-8395. DOI: 10.1021/acs.iecr.8b01239

4 D. Xiong, M. Chen and H. Li, *Chem. Commun.*, **2008**, 880-882. DOI: 10.1039/B716270G

5 J. Liang, A. Nuhnen, S. Millan, H. Breitzke, V. Gvilava, G. Buntkowsky and C. Janiak, *Angew. Chem. Int. Ed.*, 2020, **59**, 6068-6073. DOI: 10.1002/anie.201916002

6 S. A. Ullah, M. A. Azmi Bustam, A. E. Elkhalifah, N. A. Riaz, G. I. Gonfa and A. M. Mohamad Shariff, *Adv. Mater. Res.*, 2016, **1133**, 486-490. DOI: 10.4028/www.scientific.net/AMR.1133.486

7 M. Anbia and V. Hoseini, *Chem. Eng. J.,* 2012, **191**, 326-330. DOI: 10.1016/j.cej.2012.03.025

8 V. Kulkarni and S. K. Singh, *React. Chem. Eng.*, 2023, **8**, 3185-3195. DOI: 10.1039/D3RE00329A

9 S. Kayal and A. Chakraborty, *Chem. Eng. J.*, 2018, **334**, 780-788. DOI: 10.1016/j.cej.2017.10.080

10 N. A. Qasem, N. U. Qadir, R. Ben-Mansour and S. A. Said, *J. CO_2 Util.*, 2017, **22**, 238-249. DOI: 10.1016/j.jcou.2017.10.015

11 Y. Lin, C. Kong and L. Chen, *RSC Adv.*, 2012, **2**, 6417–6419. DOI: 10.1039/C2RA20641B

12 R. Zhong, X. Yu, W. Meng, J. Liu, C. Zhi and R. Zou, *ACS Sustain. Chem. Eng.*, 2018, **6**, 16493-16502. DOI: 10.1021/acssuschemeng.8b03597

13 X. H. Liu, J. G. Ma, Z. Niu, G. M. Yang and P. Cheng, *Angew. Chem. Int. Ed.*, 2015, **127**, 1002-1005. DOI: 10.1002/ange.201409103

14 M. Babaei, S. Salehi, M. Anbia, and M. Kazemipour, *J. Chem. Eng. Data*, 2018, **63**, 1657-1662. DOI: 10.1021/acs.jced.8b00014

15 S. Liu, L. T. Liu, L. X. Sun, Y. L. Zhou and F. Xu, *Polyhedron*, 2018, **156**, 195-199. DOI: 10.1016/j.poly.2018.09.033

16 P. Chowdhury, C. Bikkina and S. Gumma, *J. Phys. Chem. C*, 2009, **113**, 6616-6621. DOI: 10.1021/jp811418r